Available online at www.sciencedirect.com
SCIENCE DIRECT
Toxicology in Vitro 20 (2006) 1202–1212
Toxicology in Vitro
www.elsevier.com/locate/toxinvit

Cytotoxicity of single-wall carbon nanotubes on human fibroblasts

Furong Tian [a,*], Daxiang Cui [a], Heinz Schwarz [b], Giovani Gomez Estrada [a], Hisatashi Kobayashi [c]

[a] *Max Planck Institute for Metals Research, Heisenbergstrasse 3, 70569 Stuttgart, Germany*
[b] *Max Planck Institute for Developmental Biology, Spemannstrasse 35, 72076 Tübingen, Germany*
[c] *National Institute for Materials Science, 1-1, Namiki, Tsukuba, Ibaraki 305-0044, Japan*

Received 28 October 2005; accepted 24 March 2006
Available online 4 April 2006

Abstract

We present a toxicological assessment of five carbon nanomaterials on human fibroblast cells in vitro. We correlate the physico-chemical characteristics of these nanomaterials to their toxic effect per se, i.e. excluding catalytic transition metals. Cell survival and attachment assays were evaluated with different concentrations of refined: (i) single-wall carbon nanotubes (SWCNTs), (ii) active carbon, (iii) carbon black, (iv) multi-wall carbon nanotubes, and (v) carbon graphite. The refined nanomaterial that introduced the strongest toxic effect was subsequently compared to its unrefined version. We therefore covered a wide range of variables, such as: physical dimensions, surface areas, dosages, aspect ratios and surface chemistry. Our results are twofold. Firstly, we found that surface area is the variable that best predicts the potential toxicity of these refined carbon nanomaterials, in which SWCNTs induced the strongest cellular apoptosis/necrosis. Secondly, we found that refined SWCNTs are more toxic than its unrefined counterpart. For comparable small surface areas, dispersed carbon nanomaterials due to a change in surface chemistry, are seen to pose morphological changes and cell detachment, and thereupon apoptosis/necrosis. Finally, we propose a mechanism of action that elucidates the higher toxicity of dispersed, hydrophobic nanomaterials of small surface area.

Keywords: Cytotoxicity; Carbon nanotubes; Fibroblasts

1. Introduction

There is a clear gap in our current knowledge about the potential health effects of carbon nanotubes. The carbon nanotubes (CNTs) are seen as having a huge potential in many areas of research and application. These nanomaterials are therefore attracting investments from governments and industry in many parts of the world. The industrialization of engineered nanomaterials is advancing at a fast pace, but the risk assessment lags far behind this development. It is recently recognized that the use of nanotechnologies may raise new challenges in the safety, regulatory and ethical domains that will require scientific debate (RS/RAEng, 2004; DEFRA, 2005). In fact, the limited information available in the peer-reviewed literature suggests that CNTs possess a potential toxicity.

There are only a handful of papers about the health effects of CNTs, basically organized in two fields: exposure toxicity of CNTs to the respiratory tract (Huczko et al., 2001; Lam et al., 2004; Warheit et al., 2004; Jia et al., 2005) and dermal/epidermal toxicity (Huczko and Lange, 2001; Shvedova et al., 2003; Pantarotto et al., 2004; Ding et al., 2005; Monteiro-Riviere et al., 2005). Actually, a positive association between exposure to single-wall carbon nanotubes (SWCNTs) and pulmonary and dermal toxicity

* Corresponding author. Tel.: +49 711 689 3623; fax: +49 711 689 3610.
E-mail address: furong@mf.mpg.de (F. Tian).

0887-2333/$ - see front matter © 2006 Elsevier Ltd. All rights reserved.
doi:10.1016/j.tiv.2006.03.008

was observed from the first studies on animals. Therefore, regulatory agencies started to pay attention to the risk assessment of these novel nanomaterials. Recently, the Royal Society and the Royal Academy of Engineering, commissioned by the UK Government, issued a report (RS/RAEng, 2004) on nanotechnologies in which is admitted the many uncertainties around health, safety and environmental impact of engineered nanomaterials. A follow up report (DEFRA, 2005) identified gaps in knowledge needed to measure and characterize their risk. We are quite certain that the data currently available is insufficient for any conclusive risk assessment of nanomaterials, and further research has to be done on their toxicity in vivo, as well as their persistence and bioaccumulation (RS/RAEng, 2004; DEFRA, 2005; Stoeger et al., 2006).

The assessment is complicated because little is known about how do factors like surface chemistry, surface area, aggregation and catalytic metals in CNTs affect the cell cycle. It is assumed that these factors have a different impact on different cell types. There is, however, no systematic study that correlates toxicity to physico-chemical properties of carbon nanomaterials. The present systematic study in vitro is a step forward to fill this gap. It is known (Lam et al., 2004; Warheit et al., 2004) about effects, ranging from transient adverse reactions to granulomas formation in animal lungs, depending upon the dosage of SWCNTs. One of those works (Lam et al., 2004) studied SWCNTs with and without catalytic transition materials, e.g. with different percentage of nickel, yttrium and iron. In another study (Ding et al., 2005), the toxicological effect of two carbon nanomaterials, with different aspect ratio, were compared. It was found that multi-wall carbon nanotubes (MWCNTs) are about ten times more toxic to fibroblast cells than multi-wall carbon onions. Two studies that used SWCNTs with these catalytic metals are found in Shvedova et al. (2003) and Ding et al. (2005), in which a dose-depended toxicity of SWCNTs was used, in concentrations ranging from 0.06 μg/ml to 0.6 mg/ml. To make our results comparable to the existing literature we adopted this dose-dependent approach. It is interesting to remark that (Shvedova et al., 2003) showed that unrefined SWCNTs generate reactive oxygen species (ROS) and oxidative stress. It is thus hard to draw conclusions of the potential toxicity in vivo, generalize their results to other cell types in vitro or understand the role of catalytic transition metals.

In this paper we correlate the toxic effect of five engineered carbon nanomaterials to their physico-chemical characteristics. We show how surface area and surface chemistry impact the cell survival of human fibroblast in vitro. The refined nanomaterial showing the strongest toxic effect is taken a step further: we compare it to its unrefined version as to test whether or not catalytic transition metals enhance or decrease the toxic effect of the given nanomaterial. It is shown that catalytic transition metals, used in the production of carbon nanomaterials, influence the cell cycle of human fibroblast cells in vitro. The nanomaterials used in this research are: (i) SWCNT, (ii) active carbon (AC), (iii) carbon black (CB), (iv) MWCNT, and (v) carbon graphite (CG). A dosage-dependant analysis on human fibroblast cells was employed to be comparable to the existing literature. Fibroblast cells are important for in vitro models because one way in which these engineered nanomaterials can enter the human vascular system is through open wounds. Moreover, dermis fibroblasts cells play an important role in the cell renewing system and in maintaining the skin integrity. The in vitro model helps to assess potential toxic effects of dermal exposure to carbon nanomaterials. Since the cell cycle of fibroblast is about 24 h, we selected an exposure time of 1/2 to 2 times its cell cycle. We observed detaching and morphological changes in fibroblast cells, and analyzed these phenomena by monitoring the expression levels of extracellular matrix and adhesion-related proteins.

2. Materials and methods

2.1. Nanomaterials

Fig. 1 shows high-resolution transmission electron microscopy (HR-TEM) images of the five carbon nanomaterials: CG, MWCNT, CB, AC and SWCNT. Table 1 shows their physical dimensions, providers and surface area. The surface area was calculated as either cylinders (SWCNT and MWCNT) or spheres (CG, CB and AC). Each nanomaterial was refluxed at 120 °C in 4 M hydrochloric acid (HCl) for 19 h. The catalytic metals, i.e. iron, was removed from a group of SWCNTs by HCl. The nanomaterials were washed with water until the pH value was 6.8. They were dispersed in water by sonication (10 min) to get homogeneous suspensions. A short-term sonication does not break the nanomaterials. As an example of the purification result, we show the compositions of the refined and unrefined SWCNT surfaces, which were analyzed with a standard X-ray Photoelectron Spectroscopy (XPS) technique. The spectrum was obtained using a Concentric Hemispherical Analyser (CHA), from which the binding energy, characteristic of each element, is calculated. The binding energy of the peak is characteristic of each element: peak in energy can be used with appropriate sensitivity factors to determine the composition of surface materials. A ThetaProb equipment was used to record the XPS spectra, and monochromatic AlKα ($h\nu = 1486.6$ eV) radiation was used to generate the photoelectrons. The X-ray beam was focused to give a 400 μm spot size on the samples. The purification process is one important issue in this work because it modifies the aggregation of these engineered carbon nanomaterials. Sample spectra of the purification of SWCNTs appear in Fig. 2. The five different nanomaterials will hereafter be used in their refined form, unless otherwise indicated. Two different samples of MWCNTs, from different sources, were tested without recognizable differences for the cell survival assays. However, we did not mix them, and the source of MWCNTs we finally used appears in Table 1.

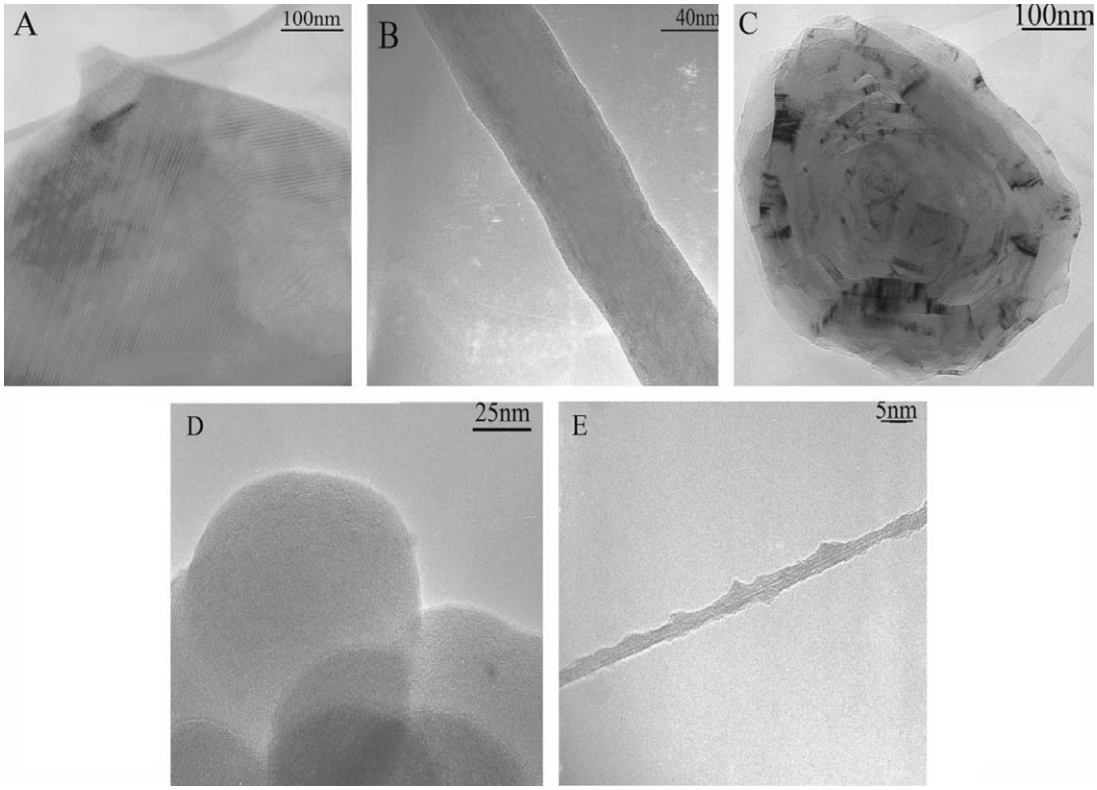

Fig. 1. High-resolution transmission electron microscopy images of the five refined carbon nanomaterials used in this research: (A) carbon graphite; (B) multi-wall carbon nanotube; (C) carbon black; (D) active carbon; (E) single-wall carbon nanotube.

Table 1
The five carbon materials that were used in our experiment

Material	Source	Dimensions	Surface area
SWCNT	Carbon Nanotechnologies, Inc. USA	2 nm × 500 nm	3.15 μm^2
AC	Silcarbon Aktivkohle, GmbH, Kirchhundem, Germany	25 nm radius	7.85 μm^2
CB	CarboTech Aktivkohle, GmbH, Essen, Germany	200 nm radius	502 μm^2
MWCNT	IIJIN Diamond Co., Ltd, Korea	50 nm × 5 μm	789 μm^2
CG	Kern group at the Max Planck Institute for Solid State Research, Stuttgart, Germany	500 nm radius	3.14 mm^2

2.2. Cell survival assay

Human dermis fibroblasts cells were cultured in a human fibroblasts medium (Cell-ling, Germany). Then, the cultured cells were incubated at 37 °C in a humidified 5% CO_2/95% air atmosphere. The cells were seeded on 96-well plates (5×10^3 cells/well), cultured for 5 h, and treated with a wide range of concentrations of SWCNT (weight/volume of solution): 0.8, 1.61, 3.125, 6.25, 12.5, 25, 50 and 100 μg/ml, from 1 to 5 days. The results from a SWCNT concentration of 25 μg/ml were compared to those cells treated with CG, MWCNT, CB and AC, from 1 to 5 days, using the same concentration. The cells treated with SWCNT were washed with phosphate-buffered saline (PBS), and stained with 3-(4,5-dimethylthiazol-z-yl)-2,5-dipheny-tetrazotium bromide (MTT). We quantified the surviving cells treated with different forms of carbon, and compared to control groups. Both necrotic and apoptotic cells were taken into account. The surviving cell colonies are expressed as percentage. The comparative plot showing the cell survival, in per cent, of all nanomaterials is presented in Fig. 3A. The result of this dosage assay of SWCNTs on fibroblast cells is shown in Fig. 3B.

2.3. Cell adhesion assay

As seen in Fig. 4, and discussed later on in Section 3.3, we focused on SWCNTs for further analyses. Cellular adhesion was evaluated according to Pucillo et al. (1993). The number of cells was determined and appropriately plated. The cells were placed on 24-well culture plates and were allowed to adhere for 5 h. Then, SWCNTs were added to the culture for 2 days. Cells were then detached with a solution of trypsin (0.06%)/ethylenediaminetetraacetate (EDTA 0.5 mM), and incubated for 15, 30, 60 and 100 min. Non adherent cells were removed by washing

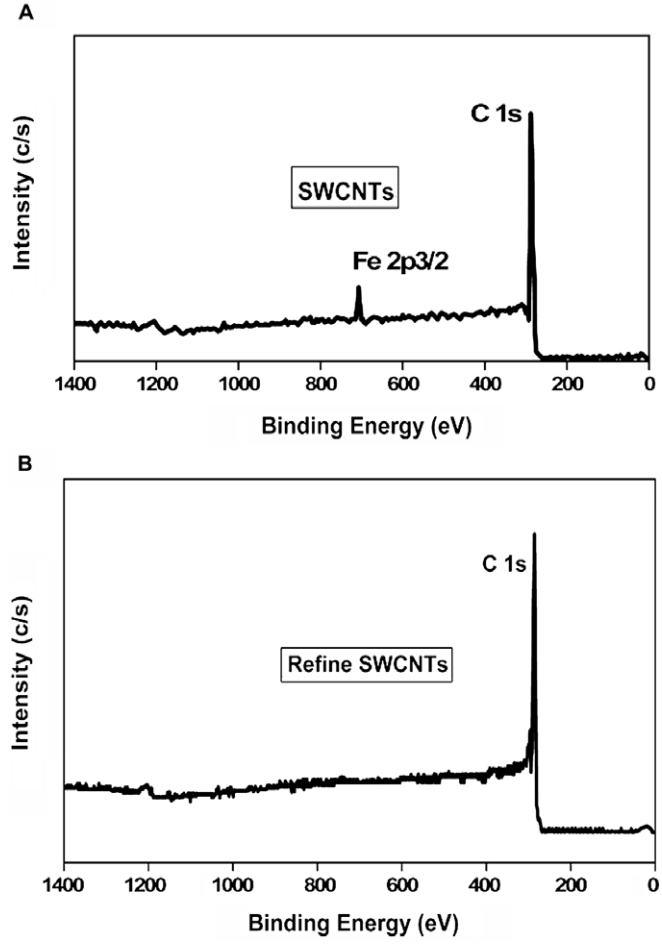

Fig. 2. Binding energy intensity of samples with and without purification process: (A) the peaks C 1s and Fe 2p 3/2 in the binding energy intensity are present in SWCNTs before purification; (B) only carbon, peak C 1s, is present in purified SWCNTs.

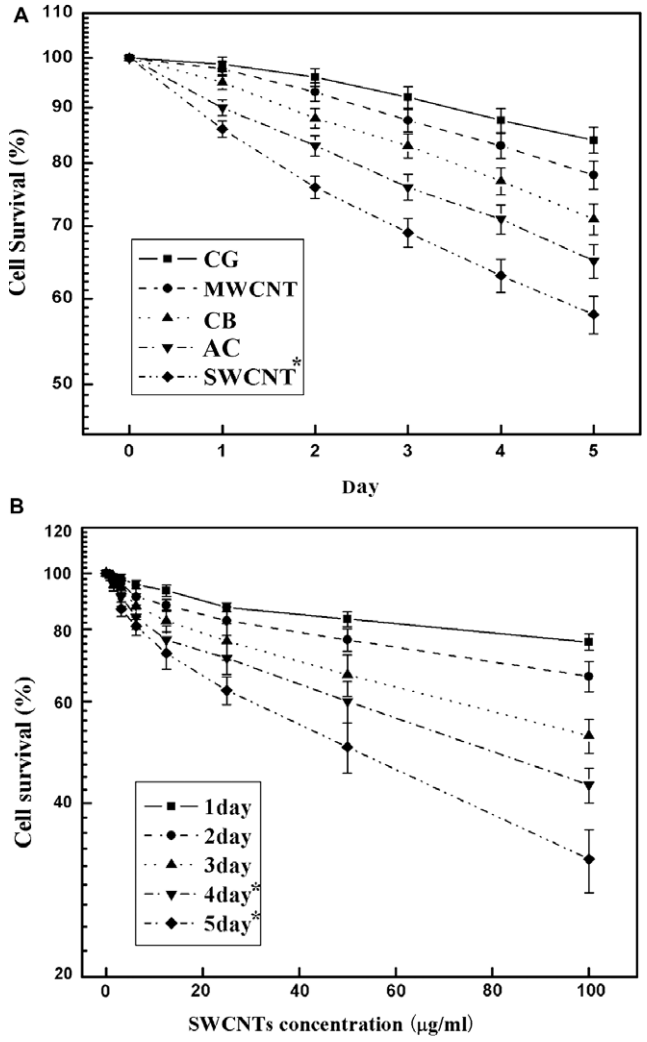

Fig. 3. The effect of refined carbon nanomaterials upon the survival of human fibroblast cells: (A) cells treated with 25 μg/ml of CG, MWCNT, CB, AC and SWCNTs, for 1–5 days. Three replicate plates were used for each data point and the experiments were performed at least three times; (B) cells treated with SWCNTs in concentrations of 0.8, 1.61, 3.125, 6.25, 12.5, 25, 50 and 100 μg/ml, for 1–5 days.

them with PBS. The attached cells were incubated for 14 days, then, they were fixed and stained with crystal violet. The number of colonies were counted and later compared to the control.

2.4. Cell death assay

Cells were treated with 25 μg/ml of unrefined SWCNT and refined SWCNT for 18 h. Dead cells were quantified by a Bio-rad Model 680 using Cellular DNA Fragmentation ELISA kit (Roche Diagnostics, Mannheim, Germany). Three replicate plates were used for each data point, and every experiment was performed at least three times. Both refined and unrefined SWCNTs had comparable surface areas. The results are discussed in Section 3.4.

2.5. Cell morphology

After incubating the human fibroblasts cells with SWCNT and the normal control cells for 48 h, they were harvested and washed with phosphate buffer (pH 7.4). Afterwards, the cells were washed with 0.01 M phosphate buffer (PBS) and fixed for 2 h by 2.5% glutaraldehyde, which was previously dissolved in PBS (pH 7.4). The cells were incubated at 37 °C for 5 min. They were embedded into 0.1% agar. This agar was fixed by 2.5% glutaraldehyde in PBS at 4 °C, for at least 2 h. The samples were washed with PBS, and then fixed by 1% osmium tetroxide at 4 °C for 2 h. Cells were dehydrated in graded series of ethanol and later embedded in epoxy resin, as described in Pucillo et al. (1993). Ultra-thin cross sections (~50 nm) of cells were observed under a Transmission Electron Microscope, Philips CM10. Cells were cultured and treated as described above. They were fixed with 2.5% glutaraldehyde in PBS at 4 °C for at least 2 h. Subsequently, these samples were washed with PBS, fixed by 1% osmium tetroxide in phosphate buffer at 4 °C for 2 h; and, dehydrated in graded series of ethanol. The cultures were analyzed with a Hitachi S-800 field emission Scanning Electron Microscope.

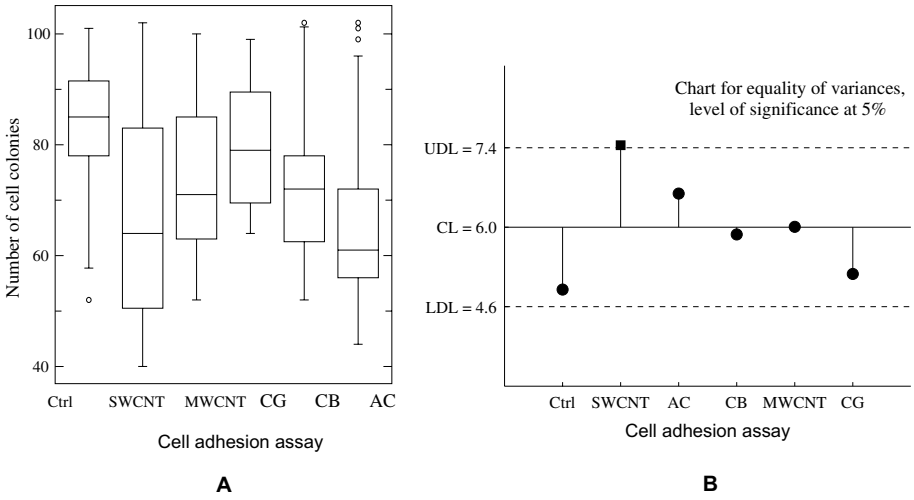

Fig. 4. Data analyses of cell adhesion and cell survival: (A) box plot showing the medians and quartiles. The outliers are represented by circles below the first and above the third quartiles; (B) a robust graphical method for testing the equality of variances. SWCNT is the only source of variance, with a level of significance at 5%. The other groups lie within the upper decision line (UDL) and lower decision line (LDL).

2.6. Immunocytochemical analysis

Immunocytochemical analysis was carried out on fibroblast cells in contact to SWCNT by using the following process. The samples were previously fixed in methanol for 20 min. They were washed with PBS and permeated with 0.2% Triton X-100 for 5 min at room temperature. Then, they were incubated with 1% normal bovine serum in PBS for 1 h. Afterwards, they were hybridized with the primary antibodies: rabbit IgG anti P-cadherin (1:2000 dilution), rabbit IgG anti FAK (1:2000 dilution) and mouse IgG anti F-actin (1:2000 dilution). The samples were washed with PBS, and incubated with sheep anti-rabbit-FITC antibody (1:160) and anti-mouse-Cy3 antibody (1:200). Their DNA was counterstained with 4′,6-diamidino-phenylindole (DAPI, 0.4 μg/ml). The cultures were mounted on *N*-propyl/gallate/glycerol and examined under a fluorescent microscope (Leica, Germany). All reagents and antibodies were purchased from Sigma Chemical Co. (St. Louis, MO).

2.7. Western blot analysis

Western blot was analyzed according to Miyakoshi et al. (2000). The cells were treated with different concentrations of SWCNTs: 0.8, 1.61, 3.125, 6.25, 12.5, 25 and 50 μg/ml, for 2 days. These cells were washed with PBS, and SWCNTs were removed afterwards. The cells were scraped from the culture dish in PBS, pH 7.4, with 100 mM 6-aminohexanoic acid, 1 mM benzamidine-HCl, and 1% Triton X-100 at 4 °C. In this study, 50 μg protein/sample was loaded in each lane. After PAGE, the polypeptides were transferred in 2 h to nitrocellulose sheets (0.45 μm pore size; from Gibco-Invitrogen) by electrophoresis (140 mA) in a Trisglycine buffer (25 mM Tris–HCl, pH 7.0; 19.2 mM glycine) containing 20% methanol. After incubating them for 30 min in PBS containing 5% skimmed milk, the nitrocellulose sheets were washed five times with PBS containing 0.1% Tween-20 (PBS-T). The seven different sheets were incubated overnight with seven different antibodies at 4 °C: (i) mouse anti-human fibronectin antibody (1:20,000 dilution), (ii) mouse anti-human laminin antibody (1:20,000 dilution), (iii) mouse anti-cyclin D3 antibody (1:5000 dilution), (iv) mouse anti-collagen-IV antibody (1:5000 dilution), (v) mouse anti-β-actin antibody (1:5000 dilution), (vi) rabbit anti-human P-cadherin antibody (1:2000 dilution), and (vii) rabbit anti-human FAK antibody (1:4000 dilution). After extensively washing them with PBS-T, the nitrocellulose sheets were incubated for 1 h with sheep anti-mouse IgG and sheep anti-rabbit IgG (1:10,000 dilutions). Immunodetection was performed using an epiluminescence (ECL) western blotting protocol kit (Amersham Life Science, UK). The immunodetected protein bands from each ECL film were analyzed by means of densitometry.

2.8. Statistical analysis

Differences between samples and the control were evaluated using the statistical analysis package SPSS 11. Statistically significance was set to $p < 0.05$. A one-way analysis of variance (ANOVA) was used to test the difference between the groups of nanomaterials. Exploratory data analyses were performed with Kolmogorov–Smirnov tests as to validate the normality assumption found in ANOVA and *t*-tests. Standard box plots and five number summaries were calculated to obtain the quartiles. The outliers were detected by looking at points far beyond first and third quartiles, i.e. outliers in Tukey's sense. A robust graphical method for testing the equality of variances (Rao and Hari, 1997), similar to analysis of means (ANOM), was used to identify those groups which are significantly different and introduce the source of variance. We considered the level of significance at 5%.

3. Results

3.1. Purification of nanomaterials

Before the purification process, the spectrum of SWCNTs shows two peaks: C 1s and Fe 2p 3/2, in Fig. 2A. The peak C 1s means carbon at 282 eV of binding energy, and Fe 2p 3/2 represents iron at 740 eV of binding energy. This result means that iron is contained in unrefined SWCNTs. On the other hand, only one peak, C 1s in Fig. 2B, appears in the binding energy intensity of SWCNTs after the purification. There is no iron in the refined SWCNTs. No other catalytic metals are seen in the spectra, e.g. Fig. 2B, of purified carbon nanomaterials. The surface areas are calculated after this purification process (Table 1).

3.2. Influence of different nanomaterials on cell survival

Fig. 3A shows the survival, from 1–5 days, of human fibroblasts cells treated with a constant concentration of 25 μg/ml: CG, MWCNT, CB, AC and SWCNT. A decreasing trend is expected over all carbon nanomaterials. At the end of the fifth day, the survival rate of cells treated with CG, MWCNT, CB, AC and SWCNT dropped to 84%, 78%, 71%, 65% and 58%, respectively. This sequence will help us to correlate toxicity and surface area in Section 4. Fig. 3B shows the survival rate of human fibroblasts in contact with SWCNTs. For example, after a treatment of 100 μg/ml of SWCNT for 1, 3 and 5 days, the cell survivals are 79%, 50%, and 31%, respectively. The survival is significantly reduced ($p < 0.05$) in the fourth and fifth days (Fig. 3B). The most pronounced effect is associated with SWCNT, the smallest nanomaterials tested, and it is closely followed by AC.

3.3. Cells adhesion assays

Fig. 4A shows a box plot of the number of cell colonies for each nanomaterial. The medians are drawn inside the boxes, and the outliers are depicted as circles far beyond the first and third quartiles. Two nanomaterials shown in this figure, SWCNT and AC, have a far lower median than the control or the remaining groups. After performing an ANOVA test we concluded that the population variances are not equal ($p < 0.05$). The source of this significant difference is identified with a robust method for testing the equality of variances through decision lines. We can observe in Fig. 4B that only SWCNT lies beyond the corresponding upper decision line (UDL), whilst all other groups are lying inside the range between the lower decision line (LDL) and UDL. Only SWCNT possesses a significant difference with respect the normal cells, and it is shown outside the decision lines, indicated with a square in Fig. 4B. We concluded that SWCNT is the only source of variance at the 5% level. These results of this section suggest a direct relationship between the surface area per material and their effect on cell survival, e.g. compare the sequence of nanomaterials in Fig. 3A and Table 1.

Interestingly, an exploratory data analysis with Kolmogorov–Smirnov tests (non-parametric, distribution free) shows that all groups, except AC, are normally distributed ($p < 0.05$). The knowledge of non-normal distributions is of vital importance. For instance, a direct pair-wise comparison of sample means via non-robust tests like the Tukey HSD test or *t*-test show a significant difference ($p < 0.05$) between AC (as well as SWCNT) and control cells (Figs. 3A and 4A). Moreover, Fig. 3A shows that AC has a number of outliers, i.e. circles beyond the third quartile, and reinforces our doubts this data is normally distributed. Therefore, these significant differences found on AC and control cells might not be reliable.

3.4. Cell death assays

The number of cell colonies decreased due to apoptosis, cell death and reduced proliferation. Three groups of cells followed an ELISA test: (i) normal cells, (ii) cells treated with 25 μg/ml of unrefined SWCNT, and (iii) cells with refined SWCNT for 18 h. We found a significant difference ($p < 0.05$) between the cells treated with 25 μg/ml of refined SWCNT and normal cells. By comparing percentile plots of refined SWCNTs and normal cells (plot not shown), we calculate that the difference starts to be significant at 30 min ($p < 0.05$), and widens thereafter. On the contrary, there was a non-significant difference between cells treated with 25 μg/ml of unrefined SWCNT and normal cells. This is the only experiment that used unrefined carbon non-material. Individual SWCNTs, from both refined and unrefined versions, have comparable surface area, but they have different surface chemistry.

3.5. Effects of SWCNTs on cell morphology

A scanning microscopy image of typical refined SWCNTs is shown in Fig. 5A. They are dispersed on the substrate and have a needle-like shape due to a high aspect ratio. The right-hand side of Fig. 5B shows a cell in contact to a bundle of refined SWCNTs, while the cell detaches from the substrate (left-hand side). Notice that some cell protuberances are not in contact with the substrate. Fig. 6A shows that membranes of normal cells did exhibit regular contours and a distinct contrast against a moderately stained cytoplasm. In contrast, cells treated with refined SWCNT showed ruffles on their cell membranes, Fig. 6B, and the cell shape appeared rounded in comparison with the normal cell. Fig. 6B also shows aggregated SWCNTs during epoxy fixation at the upper left corner of cell. SWCNTs in polymer matrices are difficult to disperse due to a lack of adhesion between the polymer and SWCNT (Park et al., 2003).

3.6. Immunostaining assays

Figs. 7A and 8A show normal cells visualized in a phase contrast microscope, in which they appeared spread and flat. Notice that P-cadherin and FAK showed a rather

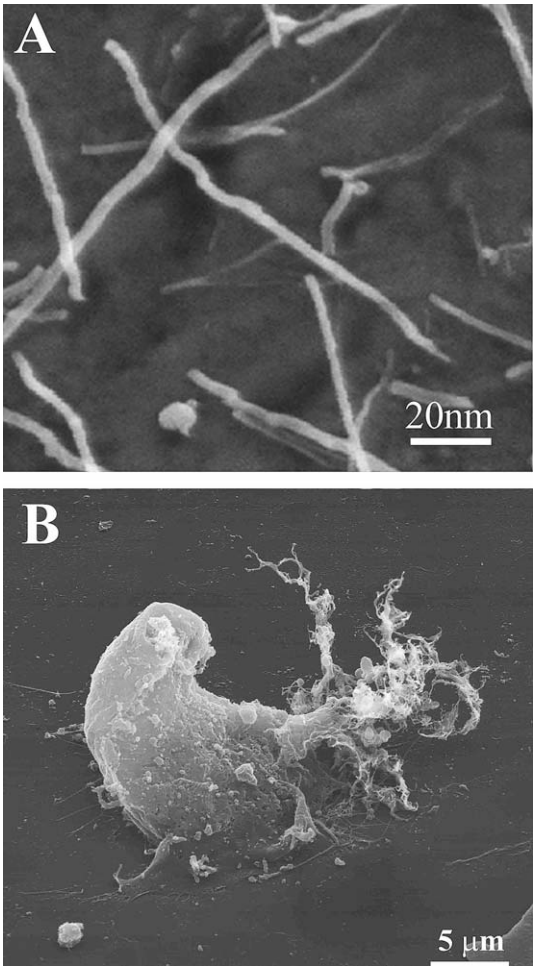

Fig. 5. Effect of SWCNTs human fibroblast cells: (A) scanning electron microscopy image of dispersed SWCNTs over the substrate, they have the sharpest shape, amid the five nanomaterials, due to a rather large aspect ratio; (B) change in cell spreading seen on samples treated with SWCNTs.

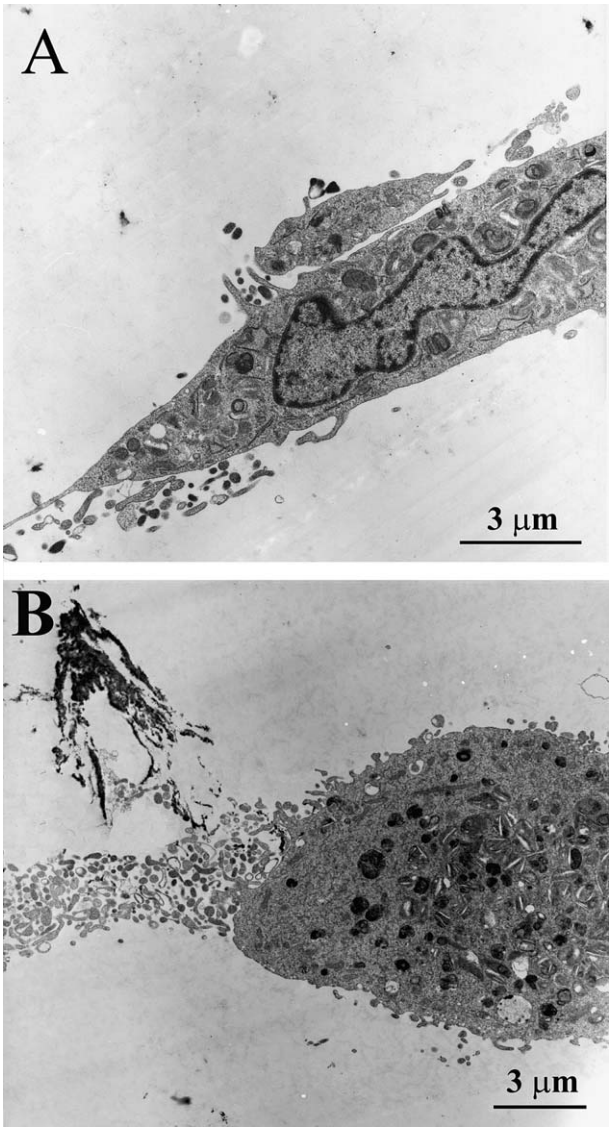

Fig. 6. Morphology of human fibroblast cells observed under transmission electron microscopy images: (A) typical normal cell; (B) cell treated with SWCNTs.

homogeneous distribution (Figs. 7B and 8B). On the contrary, cells treated with SWCNTs (Figs. 7C and 8C), had their nuclei moved towards the regions where SWCNT were attached. As their membranes and nuclei moved closer, the adhesion-related proteins exhibited a punctuate distribution along the cell periphery (Figs. 7D and 8D). Normal fibroblast cells showed a rather organized radial distribution of actin network (Fig. 9A), which turned random and irregular when treated with SWCNTs (Fig. 9B).

3.7. Western blot assays

A representative western blot analysis of different protein expression is shown in Fig. 10. This analysis focuses on the effect of SWCNTs on cell adhesion. While the concentration of SWCNTs increases from lanes 1–8, the western blot results of proteins: fibronectin, laminin and collagen IV did exhibit a strong decrease of expression levels. However, focal adhesion and cell–cell adhesion protein (FAK and P-cadherin) expressions show a less severe decreasing tendency. Cell cycle related protein cyclin D3 expression drecreas. The β-actin protein expression remained unchanged in each case. There is a significant difference ($p < 0.05$) between SWCNT groups and normal control groups.

4. Discussion

There are two main results to be discussed. Firstly, SWCNT induces the strongest adverse effect, apoptosis and necrosis, amid five refined carbon nanomaterials (Figs. 3 and 4). Secondly, refined SWCNTs are also more toxic that unrefined SWCNTs. We organize the results to explain why surface area and surface chemistry are the main variables involved in this toxic effect. While doing so, we show how our hypotheses can support a substantial body of findings on the subject.

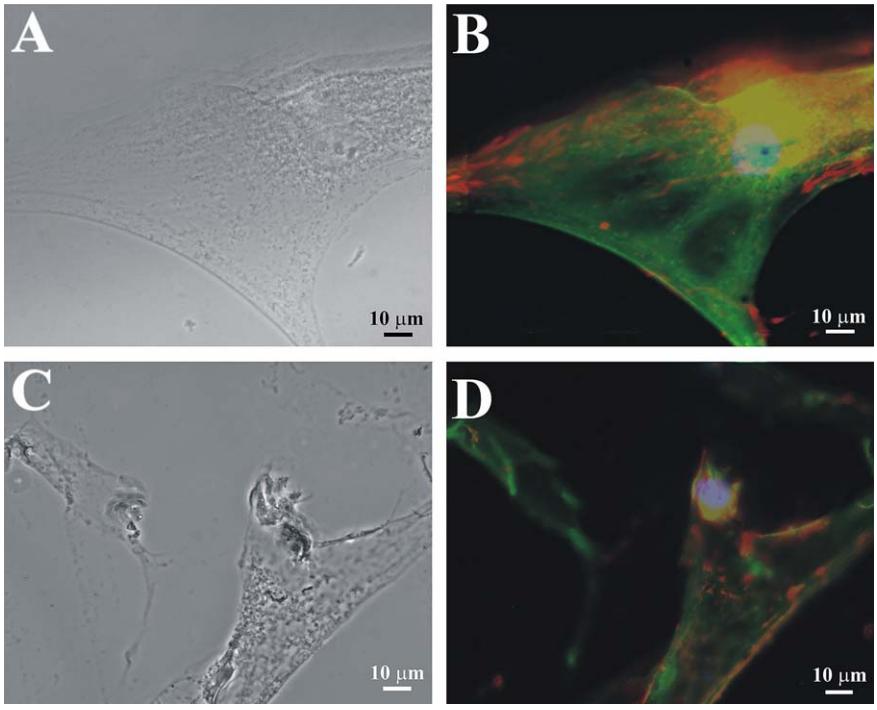

Fig. 7. Phase contrast microscopy images showing the distribution of fibronectin and P-cadherin in normal and SWCNT-treated cells: (A) normal cell; (B) fibronectin (red), P-cadherin (green) and cell nucleus (blue) of a normal cell; (C) SWCNT-treated cell; (D) fibronectin (red), P-cadherin (green) and cell nucleus (blue) of a SWCNT-treated cell. (For interpretation of the references in color in this figure legend, the reader is referred to the web version of this article.)

Our results are in stark contrast to Shvedova et al. (2003), we found that a far lower concentration (25 μg/ml) of refined SWCNT (instead of 0.06 mg/ml of unrefined SWCNTs) substantially increases cellular apoptosis or necrosis. Interestingly, SWCNTs used in Shvedova et al. (2003) contained about 30% iron (by weight), a redox-active metal. Their study highlighted the cytotoxicity of SWCNTs, and, to the best of our knowledge, it was the first peer-reviewed comparative toxicological assessment of SWCNTs. However, catalytic metals like iron and nickel are toxic (Benson et al., 2002), and hide the real toxic effect of CNTs. Thus, it is sensible to avoid the problems that arise from catalytic transition metals such as iron, nickel or cobalt by removing these materials from SWCNTs, e.g. Bahr and Tour (2002). It would be helpful to identify or isolate any potential toxic effect posed by SWCNTs per se. We observed that the cell survival has the following order: CG, MWCNT, CB, AC and SWCNT. This sequence does not correspond to the volume or aspect ratio of these nanomaterials. For instance, the aspect ration of MWCNT is 100, and the aspect ratio of SWCNT is 250, but the aspect ratio of CB and CA is 1. On the other hand, if we take the smallest physical dimension, MWCNTs should to be more toxic than CB, which is not the case. It seems that surface area is the variable that best predicts the toxicity of these nanomaterials on fibroblast cells; compare the sequences of nanomaterials in Table 1 and Fig. 3A. Surface area is a very important variable for pulmonary toxicity, and it exactly matches our cell survival assays. Independently of whether or not the significant difference of AC and control cells is reliable, see Section 3.3, this nanomaterial is certainly placed between SWCNT and CB due to its surface area (Table 1 and Fig. 3A). Each nanomaterial decreases the cell survival, but the materials with surface area of about 3.15–7.85 μm^2 had the strongest effect.

In the case of comparable physical dimensions, surface area alone does not explain why refined and unrefined SWCNTs behave differently. Morphological observations suggest a rather straightforward interpretation of this interplay of surface area and surface chemistry. Surface chemistry seems to take the leading role when the nanomaterials have comparable surface areas. Particle aggregation, due to surface chemistry and physical dimensions, also plays an important role. For instance, unrefined SWCNTs and MWCNTs are seen to group together in bundles, creating larger and thus less harmful materials. That is why, strictly speaking, only the individual SWCNTs in our experiment (Section 3.4) have comparable surface areas: the aggregated state, i.e. bundles, have a much larger surface area than any dispersed SWCNTs. Catalytic transition metals thus seem to pose a trade-off between generating ROS and oxidative stress in cells, and changing the aggregation state of carbon nanomaterials. For example, the hypothesis about bundles of unrefined SWCNTs and MWCNTs may well explain (i) why the former nanomaterial produced less severe lesions at higher doses, or (ii) why the latter nanomaterial neither induced any corneal irritation nor pulmonary damage in rodents (Huczko et al., 2001).

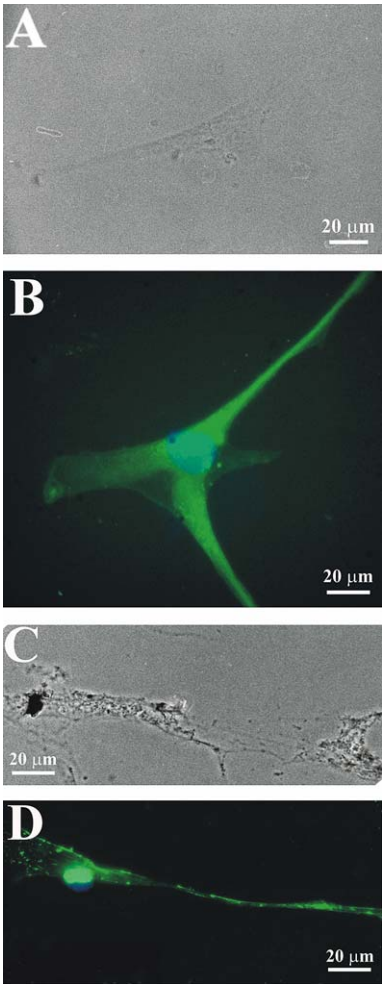

Fig. 8. Phase contrast microscopy images showing the distribution of FAK protein in normal and SWCNT-treated cells: (A) normal cell; (B) FAK (green) and cell nucleus (blue) in a normal cell; (C) SWCNT-treated cell; (D) FAK (green) and cell nucleus (blue) in a SWCNT-treated cell. (For interpretation of the references in color in this figure legend, the reader is referred to the web version of this article.)

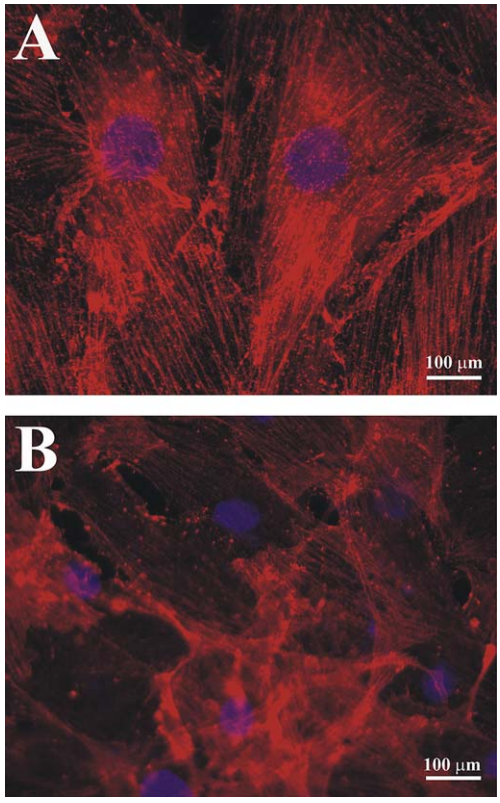

Fig. 9. Phase contrast microscopy images showing the distribution of F-actin in normal and SWCNT-treated cells: (A) F-actin (red) and cell nucleus (blue) in a normal cell; (B) F-actin (red) and cell nucleus (blue) in a SWCNT-treated cell. (For interpretation of the references in color in this figure legend, the reader is referred to the web version of this article.)

Be it on rodents or in vitro tests, aggregation and surface area support the results of Maynard et al. (2004) and Sato et al. (2005), as well as Lippmann (1994), Lam et al. (2004) and Warheit et al. (2004). Moreover, it also supports other studies that shown how chemical compounds modify the toxic effect of CNTs (Lam et al., 2004; Warheit et al., 2004), and that MWCNTs are much more toxic than carbon onions (Ding et al., 2005). Interestingly, there might be a surface area threshold in which the cellular (immune) response to hydrophobic carbon nanomaterials is similar to viral infections (Chen et al., 1998; Ding et al., 2005).

We analyzed the cell adhesion to correlate the surface chemistry of small, hydrophobic, refined nanomaterials to the morphology we observed in vitro. It is known (Pantarotto et al., 2004) that CNTs are able to cross the cell membrane and accumulate in the cytoplasm or reach the nucleus of human fibroblast cells. The underlying mechanism behind the cytotoxicity of SWCNT (or AC) could be visualized in terms of induced changes on cytoskeletons and cell morphology. It is well known that certain proteins, such as FAK, cadherin, collagen and fibronectin, play an important role in cell adhesion (Kleinman et al., 1981; Trentin et al., 2003). By focusing our experiments on these proteins, we found that western blot results are lower than normal cell expression of laminin, fibronectin, P-cadherin, FAK, collagen IV and cyclin D3 in the cells treated with refined SWCNT (Fig. 10). Carbon nanomaterials are very hydrophobic and have a high contact angle with water of about 104°. Since there are no immobilized chains on the surface of nanomaterials, it is likely that carbon nanomaterials irrupt into cell membranes by hydrophobic contact. That is why smaller hydrophobic nanomaterials, like refined SWCNT and AC, might insert ruffles to cell membranes and disturb the surface protein receptors. We observed an accumulation of FAK around cell nuclei after being exposed to SWCNTs, see Fig. 8D. There is, however, evidence that FAK is related to reduced cell proliferation and adhesion (Boateng et al., 2003; Miranti and Brugge, 2002). Our microscopy images show that SWCNTs disturb the distribution of FAK, while at the same time we observed a decrease in cell adhesion. On the other hand, cadherin is another important transmembrane protein that links the actin network to the extracellular matrix and other cells

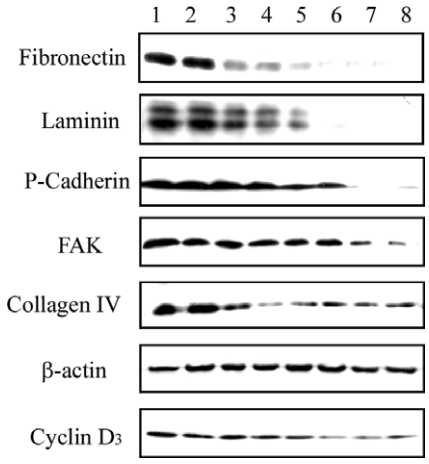

Fig. 10. Western blot analysis of the effect of SWCNTs on cell matrix adhesion-related proteins: lanes 1–8 show the expression levels of proteins in cells treated with SWCNTs with the following concentrations: 0, 0.8, 1.61, 3.125, 6.25, 12.5, 25 and 50 μg/ml, respectively.

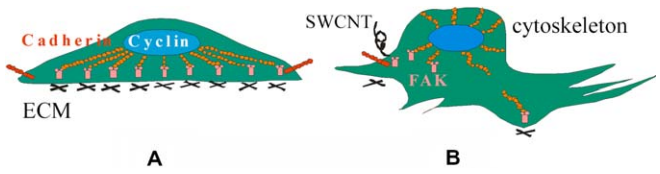

Fig. 11. A plausible mechanism for particle–cell interactions between membranes of human fibroblast cells and dispersed hydrophobic nanomaterials (e.g. SWCNT and AC) of small surface area: (A) normal cell attaching to the ECM, showing a well-spreading morphology and normal expression levels in cell matrix adhesion-related proteins; (B) dispersed, hydrophobic nanomaterial of small surface area, interacting with the cell membrane. A hydrophobic contact introduces ruffles in the cell membrane. The host cell modifies certain cell matrix adhesion-related proteins, and undergoes a morphological change in cytoskeleton and organelles, cell detachment and ultimately cellular apoptosis/necrosis.

(Miranti and Brugge, 2002). This protein rapidly responds to different cellular signals, and it is likely mediated through the cytoplasmic tail (Guilak, 1995). As a feedback, the cytoskeleton mediates intracellular signals to deform intracellular organelles (Hynes, 1999), and a decrease of cadherin expression level does result in a dramatic reduction of cadherin-mediated cell adhesion (Hendrix et al., 2003). Further, our results show that SWCNTs can disturb the distribution of both P-cadherin and factin (Figs. 7D and 8D), in full agreement to Shvedova et al. (2003). This reason might also explain why hippocampus cells did not form branches on nanotube substrates (Mattson et al., 2000).

It is known that the interactions between extra cellular matrix proteins and cyclin D3 can regulate both cell proliferation and adhesion (Nakagawa and Takeichi, 1997). All those proteins we mentioned influence the cell spreading and growth by changing the cellular structure and increasing the cellular apoptosis and necrosis. Interestingly, our present results are also consistent with previous research on different cells (HEK293) showing how SWCNTs decrease cell proliferation and adhesion and ultimately apoptosis/necrosis (Cui et al., 2005). A particle–cell model, for the mechanism of action based on changes in protein expressions is shown in Fig. 11. We propose that SWCNTs activate extra cellular matrix (ECM) protein signals, Fig. 11A, and thus the cell starts changing the cytoskeleton. Afterwards, a displacement of internal organelles and a deformation of the cell membrane take place, Fig. 11B. Then, the decrease of fibronectin, laminin, P-cadherin, FAK, cyclin D3 and collagen IV expression levels does show a notorious morphological change in shape and adhesion. That is, SWCNTs induce uneven distributions of fibronectin, P-cadherin, FAK and actin in cells (Figs. 7D, 8D, 11B), and disturb cell adhesion (Fig. 4) and spreading (Figs. 5B and 6B). That is why this phenomenon, seen in vitro, does result in cell detachment and thereupon induces cellular apoptosis/necrosis.

The toxicity of a range of refined carbon nanomaterials on human fibroblast cells in vitro was analyzed. We tested five nanomaterials exploring several dimensions and aspect ratios, as well as the unrefined version of SWCNTs. We found that refined SWCNTs have the strongest toxic effect: (i) amid five refined carbon nanomaterials, and (ii) compared to unrefined SWCNTs. That is, refined SWCNTs, i.e. without catalytic transition metals, are found dispersed and more toxic than any other nanomaterial tested. Surface area is the variable that best predicts the toxic effect amid the carbon nanomaterials. However, in the case of comparable surface areas, the surface chemistry takes the leading role. Surface chemistry modifies both the aggregation and the toxic effect of these hydrophobic nanomaterials. A mechanism describing the particle–cell interaction and the toxic effect of hydrophobic carbon nanomaterials is proposed. The mechanism of action explains why bundles of unrefined SWCNT and MWCNT are less harmful than dispersed carbon nanomaterials of small surface area. Our findings and proposed mechanism can help to remark the toxicity of dispersed carbon nanomaterials, as well as pointing out the importance of surface area, like in pulmonary toxicity. Strictly speaking, surface chemistry also changes the surface area by creating bundles of CNTs, which have larger surface area than any dispersed CNT. By comparing our results with the literature, we see evidence of an inherent toxicity of SWCNTs to fibroblast cells in vitro: with or without catalytic transition metals. A strong increase of cellular apoptosis/necrosis and detaching is associated to SWCNTs *without* catalytic metals; however, SWCNTs *with* catalytic metals are seen to induce ROS and oxidative stress. The results of our in vitro model could help to elucidate the interplay of surface area, surface chemistry and toxicity of engineered nanomaterials. Since nanotechnology is entering into large-scale use, health and safety issues of SWCNT should be promptly addressed. Therefore, further toxicological studies in vivo have to be done to assess any negative effect of engineered carbon nanomaterials upon health and environment.

Acknowledgements

We wish to thank Ms. M. Kelsch and Dr. F. Phillipp, at the Max Planck Institute in Stuttgart, for their help with HRTEM measurements; Mr. J. Berger, at the Max Planck Institute in Tübingen, for his technical assistance with SEM; as well as Prof. H. Gao and Mr. S. Coyer for their useful comments on previous versions of this manuscript.

References

Bahr, J.L., Tour, J.M., 2002. Covalent chemistry of single-wall carbon nanotubes. Journal of Materials Chemistry 12, 1952–1958.

Benson, J.M., Tibbetts, B.M., Barr, E.B., 2002. The uptake, distribution, metabolism, and excretion of methyl tertiary-butyl ether inhaled alone and in combination with gasoline vapor. Journal of Toxicology and Environmental Health A 66 (11), 1029–1052.

Boateng, S.Y., Hartman, T.J., Ahluwalia, N., Vidula, H., Desai, T.A., Russell, B., 2003. Inhibition of fibroblast proliferation in cardiac myocyte cultures by surface microtopography. American Journal of Physiology—Cell Physiology 285 (1), C171–C182.

Chen, B., Wilson, S.R., Das, M., Coughlin, D.J., Erlanger, D.F., 1998. Antigenicity of fullerenes: antibodies specific for fullerenes and their characteristics. PNAS 95, 10809–10813.

Cui, D., Tian, F., Ozkan, C.S., Wang, M., Gao, H., 2005. Effect of single wall carbon nanotubes on human HEK293 cells. Toxicology Letters 155 (1), 73–85.

DEFRA: Department for Environment, Food and Rural Affairs, UK, 2005. Characterising the potential risks posed by engineered nanoparticles. UK Government research report, London. Available from: <http://www.defra.gov.uk>.

Ding, L., Stilwell, J., Zhang, T., Elboudwarej, O., Jiang, H., Selegue, J.P., Cooke, P.A., Gray, J.W., Chen, F.F., 2005. Molecular characterization of the cytotoxic mechanism of multiwall carbon nanotubes and nano-onions on human skin fibroblast. Nano Letters 5 (12), 2448–2464.

Guilak, F., 1995. Compression-induced changes in the shape and volume of the chondrocyte nucleus. Journal of Biomechanics 28 (12), 1529–1541.

Hendrix, M.J.C., Seftor, E.A., Hess, A.R., Seftor, R.E.B., 2003. Molecular plasticity of human melanoma cells. Oncogene 22 (20), 3070–3075.

Huczko, A., Lange, H., 2001. Carbon nanotubes: experimental evidence for a null risk of skin irritation and allergy. Fullerene Science and Technology 9 (2), 247–250.

Huczko, A., Lange, H., Calko, E., Grubek-Jaworska, H., Droszcz, P., 2001. Physiological testing of carbon nanotubes: are they asbestos-like? Fullerene Science and Technology 9 (2), 251–254.

Hynes, R.O., 1999. Cell adhesion: old and new questions. Trends in Cell Biology 9 (12), M33–M37.

Jia, G., Wang, H., Yan, L., Wang, X., Pei, R., Yan, T., Zhao, Y., Guo, X., 2005. Cytotoxicity of carbon nanomaterials: single-wall nanotube, multi-wall nanotube, and fullerene. Environmental Science & Technology 39 (5), 1378–1383.

Kleinman, H.K., Klebe, R.J., Martin, G.R., 1981. Role of collagenous matrices in the adhesion and growth of cells. Journal of Cell Biology 88 (3), 473–485.

Lam, C.W., James, J.T., McCluskey, R., Hunter, R.L., 2004. Pulmonary toxicity of single-wall carbon nanotubes in mice 7 and 90 days after intratracheal instillation. Toxicological Sciences 77 (1), 126–134.

Lippmann, M., 1994. Nature of exposure to chrysotile. Annals of Occupational Hygiene 38 (4), 459–467.

Mattson, M.P., Haddon, R.C., Rao, A.M., 2000. Molecular functionalization of carbon nanotubes and use as substrates for neuronal growth. Journal of Molecular Neuroscience 14 (3), 175–182.

Maynard, A.D., Baron, P.A., Foley, M., Shvedova, A.A., Kisin, E.R., Castranova, V., 2004. Exposure to carbon nanotube material: aerosol release during the handling of unrefined single-walled carbon nanotube material. Journal of Toxicology and Environmental Health A 67 (1), 87–107.

Miranti, C.K., Brugge, J.S., 2002. Sensing the environment: a historical perspective on integrin signal transduction. Nature Cell Biology 4, E83–E90.

Miyakoshi, J., Yoshida, M., Yaguchi, H., Ding, G.R., 2000. Exposure to extremely low frequency magnetic fields suppresses X-ray-induced transformation in mouse C3H10T1/2 cells. Biochemical and Biophysical Research Communication 271 (2), 323–327.

Monteiro-Riviere, N.A., Nemanich, R.J., Inman, A.O., Wang, Y.Y., Riviere, J.E., 2005. Multi-walled carbon nanotube interactions with human epidermal keratinocytes. Toxicology Letters 155 (3), 377–384.

Nakagawa, S., Takeichi, M., 1997. N-cadherin is crucial for heart formation in the chick embryo. Development Growth & Differentiation 39 (4), 451–455.

Pantarotto, D., Briand, J.P., Prato, M., Bianco, A., 2004. Translocation of bioactive peptides across cell membranes by carbon nanotubes. Chemical Communications, 16–17.

Park, C., Crooks, R.E., Siochi, E.J., Harrison, J.S., Evan, S., Kenik, E., 2003. Adhesion study of polyimide to single-wall carbon nanotube bundles by energy-filtered transmission electron microscopy. Nanotechnology 14, L11–L14.

Pucillo, C.E., Colombatti, A., Vitale, M., Salzano, S., Rossi, G., Formisano, S., 1993. Interactions of promonocytic U937 cells with proteins of the extracellular matrix. Immunology 80 (2), 248–252.

Rao, C.V., Hari, K.S., 1997. A graphical method for testing the equality of several variances. Journal of Applied Statistics 24 (3), 279–287.

RS/RAEng: Royal Society and Royal Academy of Engineering, 2004. Nanoscience and Nanotechnologies: Opportunities and Uncertainties. Royal Society, London.. Available from: http://www.nanotec.org.uk.

Sato, Y., Yokoyama, A., Shibata, K., Akimoto, Y., Ogino, S., Nodasaka, Y., Kohgo, T., Tamura, K., Akasaka, T., Uo, M., Motomiya, K., Jeyadevan, K., Ishiguro, M., Hatakeyama, R., Watari, F., Tohji, K., 2005. Influence of length on cytotoxicity of multi-walled carbon nanotubes against human acute monocytic leukemia cell line THP-1 in vitro and subcutaneous tissue of rats in vivo. Molecular BioSystems 1, 176–182.

Shvedova, A.A., Castranova, V., Kisin, E.R., Schwegler-Berry, D., Murray, A.R., Gandelsman, V.Z., Maynard, A., Baron, P., 2003. Exposure to carbon nanotube material: assessment of nanotube cytotoxicity using human keratinocyte cells. Journal of Toxicology and Environmental Health A 66 (20), 1909–1926.

Stoeger, T., Reinhard, C., Takenaka, S., Schroeppel, A., Karg, E., Ritter, B., Heyder, J., Schulz, H., 2006. Instillation of six different ultrafine carbon particles indicates a surface area threshold dose for acute lung inflammation in mice. Environmental Health Perspectives 114 (3), 328–333.

Trentin, A.G., De Aguiar, C.B.N.M., Garcez, R.C., Alvarez-Silva, M., 2003. Thyroid hormone modulates the extracellular matrix organization and expression in cerebellar astrocyte: effects on astrocyte adhesion. Glia 42 (4), 359–369.

Warheit, D.B., Laurence, B.R., Reed, K.L., Roach, D.H., Reynolds, G.A., Webb, T.R., 2004. Comparative pulmonary toxicity assessment of single-wall carbon nanotubes in rats. Toxicological Sciences 77 (1), 117–125.